Korea-Australia Rheology Journal
Vol. 15, No. 1, March 2003 pp. 43-50

Properties and particles dispersion of biodegradable resin/clay nanocomposites

Kenji Okada*, Takashi Mitsunaga and Youichi Nagase
Department of Chemistry and Bioscience, Kurashiki University of Science and The Arts, 2640 Nishinoura Tsuragima-cho, Kurashiki 712-8505, Japan

(Received December 29, 2002)

Abstract

In this study, two types of biodegradable resins-based clay nanocomposites, in which organic montmorillonite clay was filled, were prepared by the direct melt blending method. In order to characterize the nanocomposite structure, wide-angle X-ray diffraction (WAXD) and TEM observation were performed. Characterization of the nanocomposites shows that intercalated and partially exfoliated structures were generated by the melt blending method. Mechanical and rheological properties of the nanocomposites were measured respectively. For the mechanical properties, there were improvements in tensile strength and Young's modulus of the nanocomposites due to the reinforcement of nanoparticles. The rheological behaviors of the nanocomposites were significantly affected by the degree of the dispersion of the organoclay. The storage modulus of the nanocomposites was measured and the degree of the dispersion of the organoclay was evaluated from the value of the terminal slope of the storage modulus. In addition, the quantity of the shear necessary for making the nanocomposite for melt intercalation method was estimated from the relationship between the value of the terminal slope of the storage modulus and the applied shear.

Keywords : nanocomposite, biodegradable resin, mechanical strength, rheological properties, shear strength, particle dispersion

1. Introduction

Biodegradable resin has been expected to minimize the environmental impact of plastics and to develop sustainable plastics. However, the properties of biodegradable resin are inferior to general commodity plastics and plastic unit price is high, and thus there are many yet problems to be solved on the utilization of the biodegradable plastics.

Recently, polymer-clay nanocomposites have generated enormous interest due to their dramatic improvements in material properties (mechanical, thermal and barrier properties) with a small amount of clay. Since Kojima *et al.* (1993) reported that the material properties of nylon-based clay nanocomposites are drastically improved, the development of the nanocomposite to various resins is being attempted (Carrado, 2000; Lebaron *et al.*, 1999). Though there is the first report of polycaprolactone-clay nanocomposite on the application of the biodegradable resin by Messersmith *et al.*(1995), the application to the biodegradable resin is relatively less than commodity plastics (Mitsunaga *et al.*, 2002; Ray *et al.*, 2002).

In this study, biodegradable resin based nanocomposites are prepared by directly blending the clay into the polymer, and physical properties of the composite are examined. The degree of the shear necessary for making nanocomposites is estimated from the rheological properties of the nanocomposites.

2. Experimental

2.1. Materials

Montmorillonite clay is commonly used as a filler of polymer-clay nanocomposites because layered silicate platelets of the clay can exfoliate as nanoparticles. However, the surface of the silicate platelets is originally hydrophilic and thus it must be modified by organic treatments to make the platelet compatible with the polymer. In this study, organically modified montmorillonite clay (organoclay) with trimethyl octadecyl ammonium cation was used as the filler (commercial grade: S-BEN-E, Hojyun). In this study two kinds of the biodegradable resins (PCL: polycaprolactone and PBS: polybutylene succinate) were used as a matrix polymer. The properties of these biodegradable resins are shown Table 1. PCL and PBS resins were respectively grafted in maleic anhydride in order to more increase compatibility with the filler. A detailed experimental procedure of the grafting reaction can be found by our previous study (Mitsunaga *et al.*, 2002).

*Corresponding author: okada@chem.kusa.ac.jp

Table 1. Properties of biodegradable resin used in this study

Resin (Source)	Commercial grade	Density [kg/m^3]	Melting point [°C]	Weight average molecular weight
PCL: polycaprolactone (Daicel Chemical Industry Ltd.)	PH7	1.14×10^3	53	$\sim7\times10^4$
PBS: polybutylene succinate (Showa Highpolymer Co. Ltd.)	#1003	1.26×10^3	116	$\sim1\times10^5$

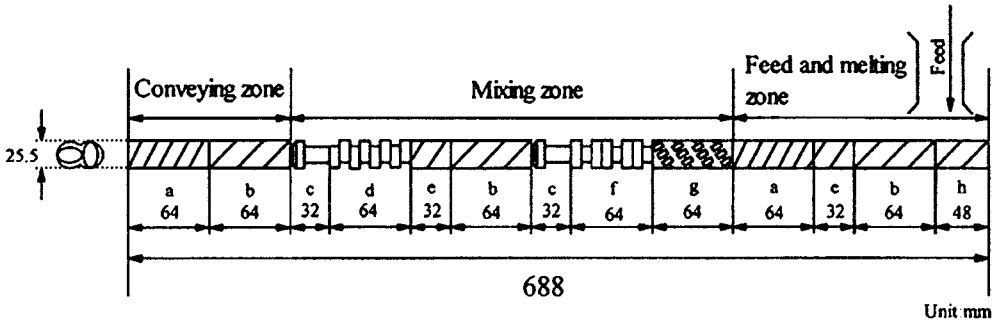

a: two lobe screw (pitch 12mm)
b: two lobe screw (pitch 24mm)
c: seal disk
d: two lobe disk
e: two lobe screw (pitch 16mm)
f: three lobe disk
g: two lobe screw (reversely lead with square groove, pitch 16mm)
h: two lobe screw (pitch 24mm)

Fig. 1. Screw configuration of a twin-screw extruder.

2.2. Nanocomposites preparation

Polymer nanocomposites have been prepared using various methods such as in situ polymerization, emulsion polymerization and melt intercalation (Chujo, 2002). One of the alternative methods is the melt intercalation method in which the clay is directly blended with the polymer. The preparation of the polymer-clay nanocomposite was carried out using a biaxial and segmental extruder (Model 2D25W, Toyo Seiki). The configuration of the twin-screw extruder is shown in Fig. 1. The screw has been composed of three zones: feed and melt, mixing, and conveying division. In the mixing zone lobe disk and lobe screw with the reverse lead angle groove were set to achieve the strong mixing efficiency. The process condition of the twin-screw extruder for making the biodegradable polymer-clay nanocomposites is shown in Table 2. An internal mixer (Model NR-PM3, Nihon Rheol. Equip.) was also used to prepare the nanocomposites in order to examine the effect of the shear on the degree of dispersion of the organoclay in the polymer matrix. The mixer was equipped with a mixing blade of roller type (capacity: 100 mL).

2.3. Characterization methods

Wide-angle X-ray diffraction (WAXD) measurements for the nanocomposite were performed using an X-ray diffractometer (Model RINT 2500V, Rigaku), in order to determine the degree of clay platelets separation. The analysis was run from the diffraction angle $2\theta=2-10^\circ$ at a rate of 2°/min. The morphology of the nanocomposite samples was observed by transmission electron microscopy (TEM) operated at 200 kV (Model EM-002B, Topcon). The ultramicrotomy technique was adopted to prepare ultrathin sections of the sample for observation in the TEM using a Reichert Ultracut.

Table 2. Operating conditions of twin screw extruder for making biodegradable polymer-clay nanocomposites

Resin	Temperature [°C]	Revolution speed [r.p.m.]	Resident time [min.]
PCL	130	55	4
PBS	150	55	4

2.4. Mechanical and rheological tests

The extruded nanocomposite samples were pelletized and then the pellets were injection molded for making the test specimens of mechanical test using a 40-ton injection machine (Model PS40F5E, Nissei Plastic Industry). The condition of the injection molding for making the test specimens is shown Table 3. The tensile test of the samples was carried out according to JIS K7113 using a tensile test machine (Model PS-500, JT Tohsi). All rheological properties of the samples were measured using a rheometer (model RD-152S, Nihon Rheol. Equip), with cone and plate geometry in oscillatory mode. The plates had a diameter of 21.5 mm and a cone angle of 1° and 0.34°, respectively.

Table 3. Conditions of injection molding

Resin	Injection pressure [MPa]	Injection speed [mm/s]	Injection time [sec]	Cylinder temperature [°C]	Mold temperature [°C]
PCL	155	97.6	10	130	25
PBS	146	61	10	150	25

2.5. Experiment of particles dispersion

In order to examine the effect of the shear on the degree of dispersion of the organoclay, firstly conventional composites were prepared by the internal mixer. Subsequently the samples were sheared at a steady shear mode using the rheometer. After steady shear was applied, rheological measurements of the samples were carried out and the dispersion state was examined.

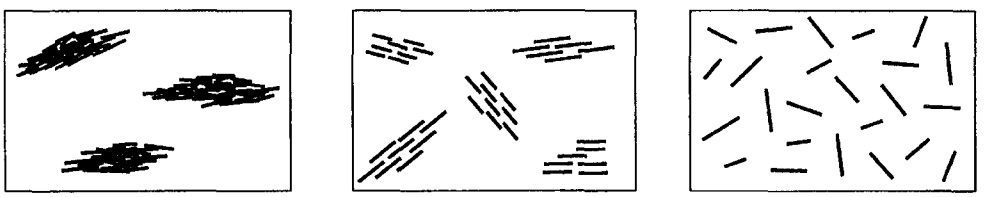

Fig. 2. Possible polymer-clay nanocomposite structures.

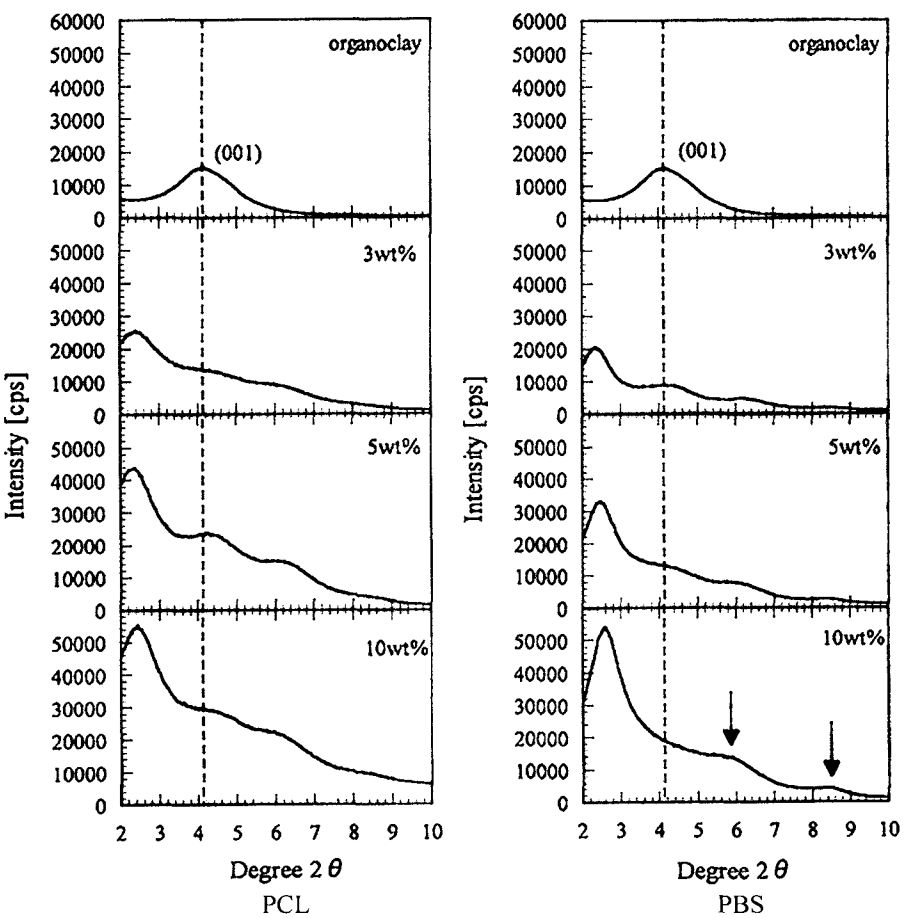

Fig. 3. WAXD patterns for organoclay and nanocomposite samples. The dashed line shows the peaks of original organoclay reflection.

3. Results and discussion

3.1. Structure of biodegradable resin-clay nanocomposites

In general, two types of polymer-clay nanocomposites are possible during the melt intercalation process. When organoclay is blended into the polymer and the silicate layers do not separate, they are referred as a conventional composite. Intercalated nanocomposite, in which polymer enters the clay galleries and causes the platelets apart less than 20Å to 30 Å separations. Exfoliated nanocomposite, in which the silicate layers are delaminated and dispersed well in the polymer matrix (LeBaron *et al.*, 1999) (see Fig. 2). Fig. 3 shows the results of WAXD analysis of the nanocomposites prepared by the extruder. The WAXD pattern of the original organoclay shows the peak of intensity at the diffraction angle of $2\theta=4.2^{\circ}$ and the equivalent distance of silicate layer (d-spacing) is 19.9Å. The intensity peaks of the nanocomposites changed to the smaller angle ($2\theta \leq 2.5^{\circ}$) and the value of d-spacing increased (d=34–38 Å). This shift of the WAXD peak toward lower value of 2θ indicates that the intercalation of the polymer chain expanded the clay galleries and the intercalated structure was generated during the compounding process. However, for PBS-clay nanocomposites (10 wt% organoclay content) there are peaks at larger position than that of the original organoclay (arrow ↓). These peaks seem to come from the formation of tactoids that were compressed the compounding process.

TEM images observed for the same samples as those shown in WAXD analysis are shown in Fig. 4. Fig. 4 shows a TEM image of PBS-nanocomposite (5 wt% organoclay content). This image shows that stacks of intercalated clay platelets and individual exfoliated platelets are embedded in the polymer matrix. TEM images for both nanocomposites (PBS and PCL) at higher magnification are shown in Fig. 5(a) and (b), respectively. The presence of the intercalated stacks with less than 10 numbers platelets can be appreciated in Fig. 5(a) and (b).

3.2. Mechanical properties

The results of the mechanical properties for the nanocomposites prepared by the extruder are shown in Figs. 6 and 7, respectively, as a function of the organoclay concentration. When the organoclay was added, a significant improvement in the tensile strengths for both the nanocomposites samples is observed up to 5 wt% organoclay loading. This may come from the reinforcement effect of the high aspect ratio of the intercalated clay particles. At 10 wt% concentration the organoclay loading is less effective. The more addition of the organoclay seems to generate tactoids that reduce the reinforcement effect of the filler. The addition of the hard particles such as the organoclay has a

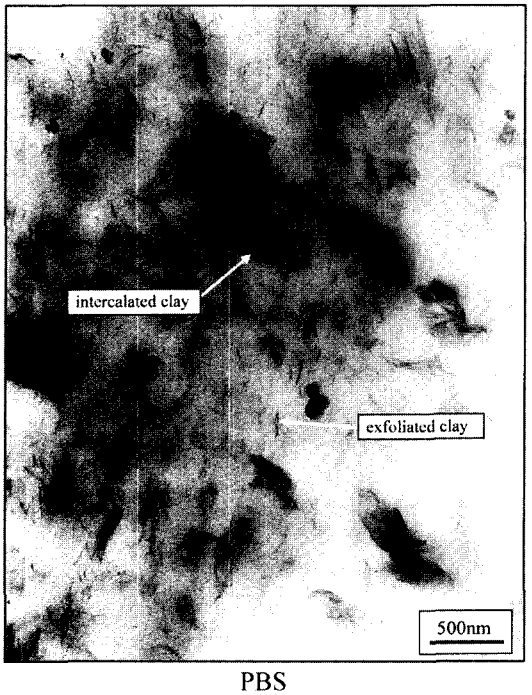

PBS

Fig. 4. TEM image of PBS-clay nanocomposite (5 w% organoclay content) prepared by the extruder.

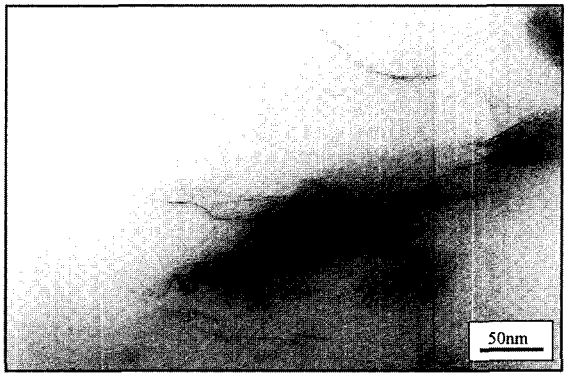

(a) PBS

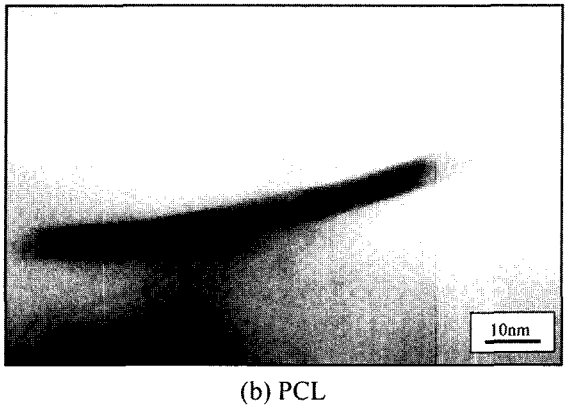

(b) PCL

Fig. 5. Intercalated structures of organoclay on nanocomposite samples.

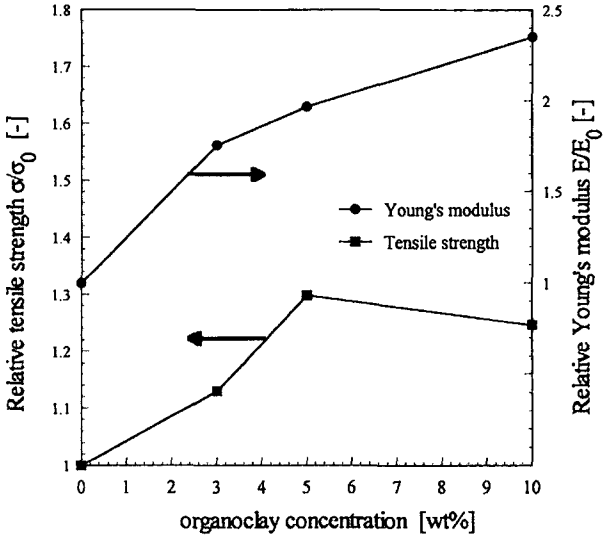

Fig. 6. Mechanical properties of PCL-clay nanocomposites as a function of organoclay concentration. Neat PCL: σ_0=11.9 MPa, E_0=47.5 MPa.

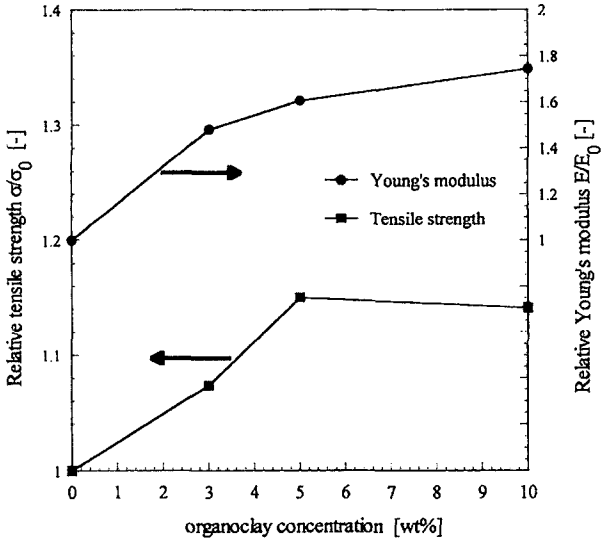

Fig. 7. Mechanical properties of PBS-clay nanocomposites as a function of organoclay concentration. Neat PBS: σ_0=27.3 MPa, E_0=63.8 MPa.

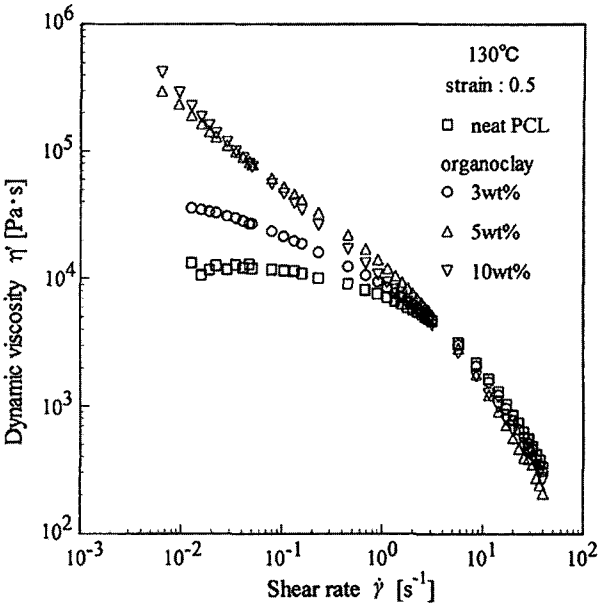

Fig. 8. Shear viscosity behavior of PCL-clay nanocomposites.

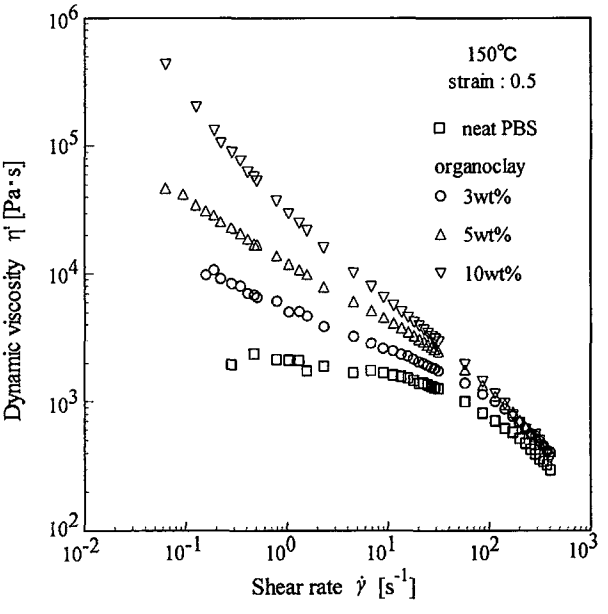

Fig. 9. Shear viscosity behavior of PBS-clay nanocomposites.

much higher modulus than the polymer matrix, which increase the composite modulus. Figs. 6 and 7 also show that Young's modulus of the nanocomposite samples increases as the organoclay concentration increases.

3.3. Rheological properties

The shear viscosity behavior (η') for the extruded nanocomposites are shown in Figs. 8 and 9, respectively. The neat PBS and PCL resins exhibit Newtonian plateau at low shear rate and display a shear-thinning behavior at high shear rate. For both nanocomposites the plateau behavior in low shear rate region disappears and the values of η' at low shear rate rapidly increases as the organoclay concentration increases. The nanocomposites also display the shear-thinning behavior in high shear rate region. This seems to originate from the alignment of the intercalated organocay particles by the applied shear. In general, polymer-clay nanocomposites show a high dependency of the shear strain because of the high aspect ratio of the clay platelets. Fig. 10 shows the dependency of the strain on the viscosity of the nanocomposites. It can be seen that the nanocomposites show the larger dependency of the strain on the viscosity, compared with those for neat resins. Figs. 11 and 12 show the storage modulus (G') of these nanocomposites,

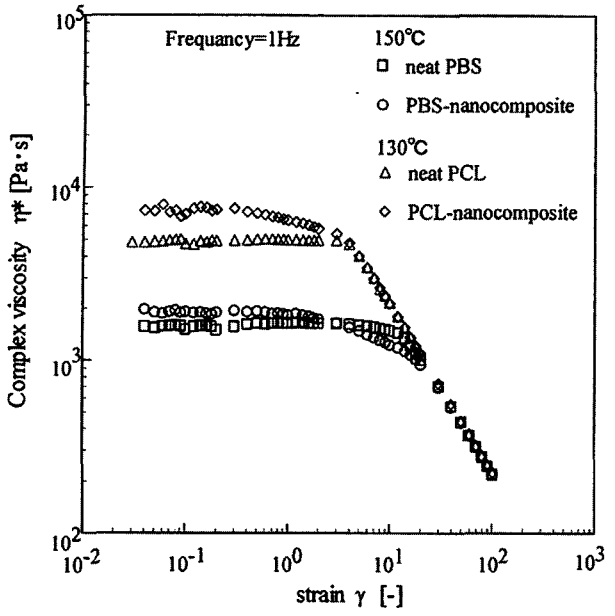

Fig. 10. Dependency of strain on the complex viscosity (η^*) for nanocomposite sample (5 wt% organoclay content).

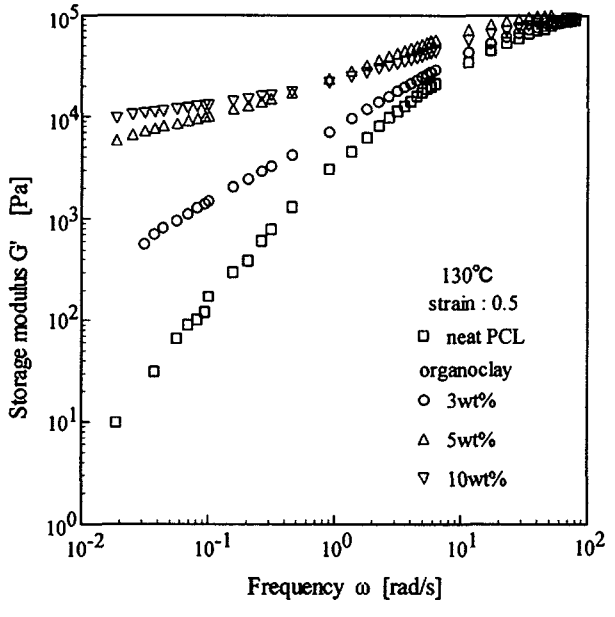

Fig. 11. Storage modulus (G') of PCL-clay nanocomposites.

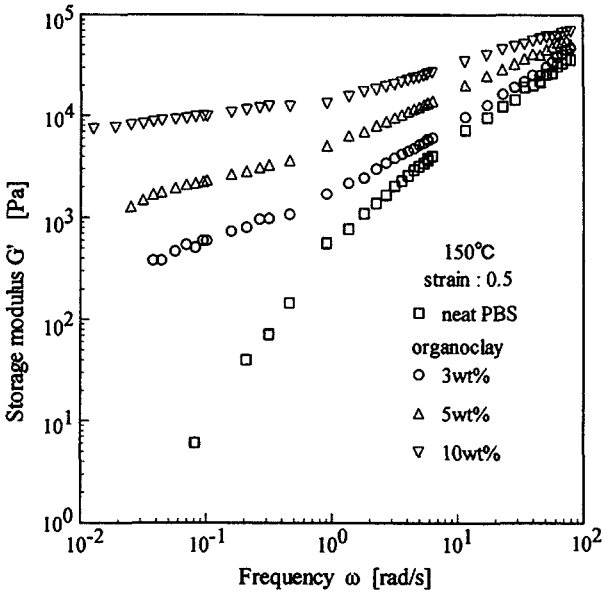

Fig. 12. Storage modulus (G') of PBS-clay nanocomposites.

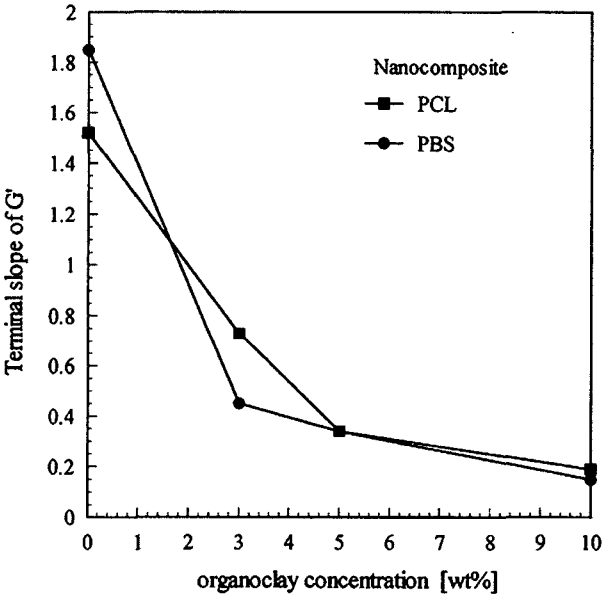

Fig. 13. Plots of terminal slope of G' vs. organoclay concentration.

respectively. The curves of G' for both the samples show monotonic increase as the organoclay concentration increases at all frequency. In addition, the slope of G' at a very low frequency decreases with increasing the organoclay loading. This low-frequency response of G' is indicative of a "pseudo-solid-like" behavior which is attributed from the strong interactions between the dispersed clay platelets and the polymer as the organoclay concentration increases. A similar rheological response at low frequency has been reported for polypropylene/clay nanocomposites system by Koo *et al.* (2001). They reported that the change of terminal slopes (the slope of G' at low frequency) depends not only on the clay concentration but also on the morphology of the nanocomposites. Therefore, it is considered that the value of the terminal slope of G' can be interpreted as an index that represents the degree of the dispersion of the polymer-clay nanocomposites. Fig. 13 shows the values of the terminal slopes of G' estimated for the data shown in Figs. 11 and 12, as a function of the organoclay concentration. It can be seen that the values of the terminal slopes of G' for both samples drastically

decrease with increasing the organoclay concentration but the change of terminal slopes of G' are small between 5-10 wt% organoclay content. This result seems to indicate that the degree of the clay dispersion decreases with increasing clay content. You should also notice that the dependency of the terminal slope of G' on the addition of the organoclay is similar to the result on the tensile strength shown in Figs. 6 and 7.

3.4. Effect of shear on the dispersion

Melt intercalation method using the extruder has been expected as a useful technique because of its high potential for making polymer-clay nanocomposites. However, few reports have explored the effect of the shear by the extruder for making nanocomposites (Dennis and Hunter, 2001). In order to clarify the effect of the shear on the melt intercalation method, the relationship between the shear and the terminal slope of G' was examined. The samples were prepared by the internal mixer under the weak shearing conditions (mixing speed: 16 rpm, mixing time: 13 min). Then various steady shears were applied to the samples using the rheometer. Fig. 14 shows the effect of the applied shear on the storage modulus for PBS-clay nanocomposite (5 wt% organoclay content). From the result of Fig. 14, it can be seen that the value of G' in the low frequency region increases with increasing the applied shear rate ($\dot{\gamma}_{ap}$). Fig. 15 shows the results of WAXD patterns measured for the same samples as those shown in Fig.14. The WAXD pattern shows that the intensity peak on the intercalated structure increases with increasing $\dot{\gamma}_{ap}$. These results of Figs. 14 and 15 indicate that the degree of dispersion of the organoclay increases with increasing $\dot{\gamma}_{ap}$. Fig. 16 shows the plots of the terminal slope of G' vs. $\dot{\gamma}_{ap}$ for the nanocomposites. The data, which changed the time of the shear, is also shown in the figure. From the result of Figs. 16, it can be found that there is a critical shear rate in which the clay dispersion is not effective (in this case $\dot{\gamma}_c \cong 100s^{-1}$) and over the shear rate of $\dot{\gamma}_c$ the dispersion of the clay progresses in proportion to $\dot{\gamma}_{ap}^{-0.35}$ with independent of the time of the shear. Furthermore, in Fig.16 the value of the

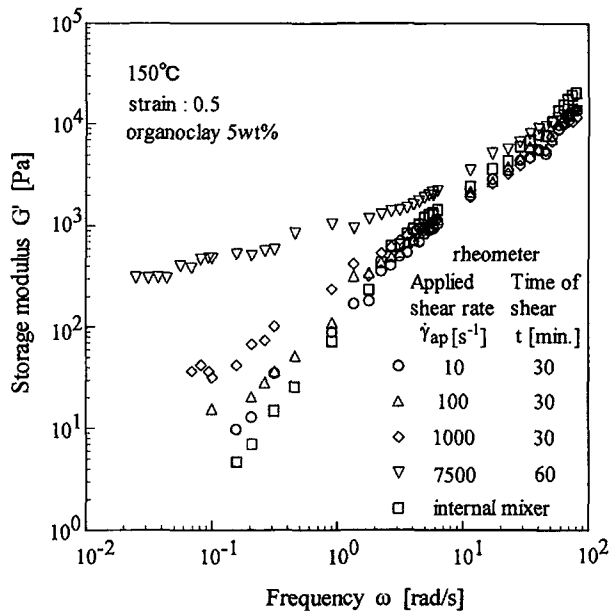

Fig. 14. Change of the storage modulus (G') for PBS-clay nanocomposites applied various shear using a rheometer.

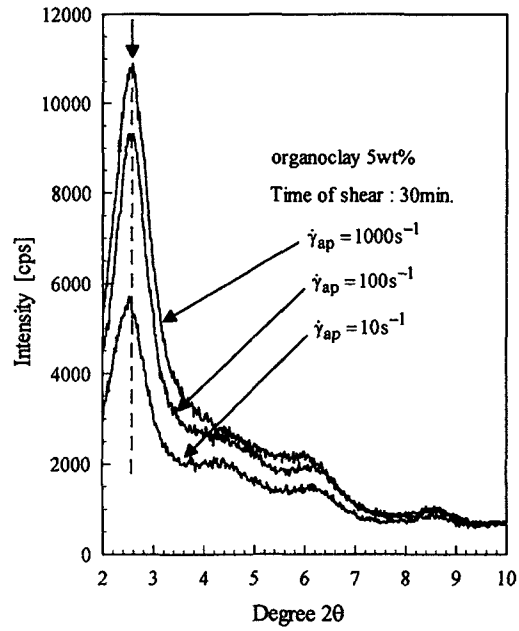

Fig. 15. WAXD patterns for PBS-clay nanocomposites applied various steady shear rate. The arrow shows the peak location on the intercalated structure.

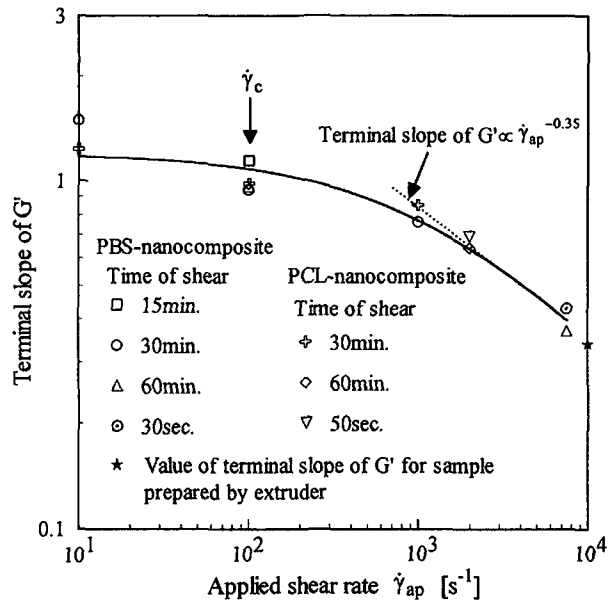

Fig. 16. Plots of terminal slope of G' vs. $\dot{\gamma}_{ap}$.

terminal slope of G' for the nanocomposite prepared by the extruder is also shown. From the relationship between the terminal slope of G' and $\dot{\gamma}_{ap}$, it is possible to estimate the quantity of the shear necessary for making PBS-clay nanocomposite (5 wt% organoclay content) is about $\dot{\gamma}_{ap} \cong 10^4 s^{-1}$.

4. Conclusions

Biodegradable polymer-clay nanocomposites based on PCL and PBS resins were effectively produced by the twin-screw extruder with the montmorillonite-based organoclay. From the results of WAXD analysis and TEM observation for the nanocomposites, it was found that the nanocomposites of intercalated and partially exfoliated types were generated by the direct melt blending method. The mechanical and rheological properties of the nanocomposites were measured, respectively. For mechanical properties, it was found that there were improvements in tensile strength and Young's modulus due to the reinforcement effect of the intercalated clay particles. The shear viscosity behavior of the nanocomposites showed drastic increase in the viscosity at low shear rate region and showed a large dependency of the strain due to the alignment of the clay platelets. The increase of the storage modulus was observed at low frequency region, suggestive of a solid-like response, which is attributed to the presence of the intercalated clay particles. It was found that there is a critical shear rate in which the clay dispersion is not effective, and that the quantity of the shear necessary for making the nanocomposite for melt intercalation method was expected from the relationship between the value of the terminal slope of the storage modules and the applied shear.

List of symbols

E_0 = Young's modulus of neat polymer [MPa]
E = Young's modulus [MPa]
G' = storage modulus [Pa]
γ = strain [–]
$\dot{\gamma}$ = shear rate [s^{-1}]
$\dot{\gamma}_{ap}$ = applied shear rate [s^{-1}]
$\dot{\gamma}_c$ = critical shear rate [s^{-1}]
η' = dynamic viscosity [Pa·s]
η^* = complex viscosity [Pa·s]
σ_0 = tensile strength of neat polymer [MPa]
σ = tensile strength [MPa]
ω = frequency [rad/s]

References

Carrado, K. A., 2000, Synthetic organo- and polymer-clays: preparation, characterization, and materials applications, *Applied Clay Science* **17**, 1-23.

Chujo, K., 2002, Recent situation of polymer nanocomposites, *J of JSPP* **14-4**, 200-205.

Dennis, H. R. and D.L. Hunter, 2001, Nanocomposites: The importance of processing, *Plastic Eng.* January, 56-60.

Kojima, Y., A. Usuki, M. Kawasumi, A. Okada, Y. Fukushima, T. Kurauchi and O. Kamigaito, 1993, Synthesis of nylon 6-clay hybrid, *J. Mater. Res.* **8**, 1179-1184.

Koo, C. M., M. J. Kim, M. H. Choi, S. O. Kim and I. J. Chung, 2001, Rheology and crystallization behaviors of maleated polypropylene/clay nanocomposites, *Proc. of PPS-17* Montreal, Canada, Symposium **1**, 1-14.

LeBaron, P. C., Z. Wang and T. J. Pinnavaia, 1999, Polymer-layered silicate nanocomposites: an overview, *Applied Clay Science* **15**, 11-29.

Messersmith, P. B. and E. P. Giannelis, 1995, Synthesis and barrier properties of poly(ε-caprolactone)-layered silicate nanocomposites, *J. Poly. Sci.* Part A Polym. Chem. **33**, 1047-1057.

Mitsunaga, T., K. Okada, Y. Nagase and T. Kimura, 2002, Modification of biodegradable resin by clay nanocomposite, *J. of JSPP* **14-9**, 604-610.

Ray, S. S., M. Okamoto, K. Yamada and K. Ueda, 2002, New and nobel biodegradable polyactide-layered silicate nanocomposites: preparation, materials properties and melt rheology, *Proc. of PPS-2002* Taipei, Taiwan Symposium, **9**, 1-5.